

A Radiating Monolithic Integrated Planar Oscillator at 55 GHz

A. Stiller, K. M. Strohm, E. Sasse, E. Biebl, and J.-F. Luy

Abstract—A planar radiating oscillator consisting of a planar resonant antenna and an IMPATT diode monolithically integrated on a silicon substrate is presented. This oscillator finds various applications in low-cost sensors, e.g., velocity sensors. The design tools are discussed and the calculated results are compared to measurements.

I. INTRODUCTION

MONOLITHIC millimeter wave integrated transmitters and receivers are key elements of sensor systems for automotive applications. These sensor systems may be used for speed measurement, side crash detection or evaluation of road conditions. The transmitters may consist of an active element such as an IMPATT diode and an integrated resonant structure. In order to minimize the required chip dimensions, the resonator simultaneously acts as an antenna. The lack of additional microstrip lines for connecting the oscillator to an external antenna reduces parasitic losses to a minimum [1]. But matching of the low-impedance IMPATT diode in a planar configuration is critical and requires careful optimization of diode structure, geometry, and resonator layout. By use of resonator layouts based on planar asymmetric dipole antennas [2], the impedance requirements are met. This impedance was previously determined by on-wafer measurements of various IMPATT diodes. Dipole antenna and IMPATT diode have been monolithically integrated on high resistive silicon with a thickness of 100 μm . This small substrate thickness results in high thermal stability of the oscillator. With such an integrated IMPATT diode transmitter, a radiated output power of 6 dBm at 55.27 GHz has been achieved.

II. ACTIVE ELEMENT DESIGN

Fig. 1 shows the doping profile of the employed quasi read double drift IMPATT diode (QRDD) [3]. The design is slightly modified with respect to the introduction of a diffusion buffer in order to compensate for an outdiffusion of the boron-doped buried layer. The n^+ spike leads to a confinement of the avalanche region with beneficial impact on the impedance

Manuscript received August 25, 1995. This work was supported by the Bundesministerium für Bildung, Wissenschaft, Forschung und Technologie under project number 01M2938A8.

A. Stiller is with Lehrstuhl für Hochfrequenztechnik, Technische Universität München, 80333 München, Germany, and Daimler-Benz Research, 89081 Ulm, Germany.

K. M. Strohm, E. Sasse, and J.-F. Luy are with Daimler-Benz Research, 89081 Ulm, Germany.

E. Biebl is with Lehrstuhl für Hochfrequenztechnik, Technische Universität München, 80333 München, Germany.

Publisher Item Identifier S 1051-8207(96)00910-5.

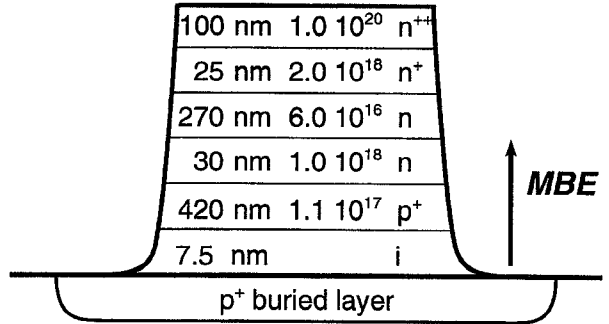


Fig. 1. Doping profile of the QRDD type IMPATT diode.

level and the conversion efficiency, respectively. The complete layer sequence was grown by silicon molecular beam epitaxy (Si-MBE). The device with a diameter of 22 μm is processed following a published SIMMWIC process [4]. The impedance of the QRDD IMPATT diode was measured up to 50 GHz by means of network analyzer (NWA) attached to a CASCADE wafer prober. To minimize the influence of the measurement setup on the diodes a constant leveled NWA output power of -27 dBm was used. During the measurements the IMPATT diodes were operated as one port amplifiers. In the frequency range from 50–60 GHz the impedance of the QRDD diode has been extrapolated on basis of the measurements (Fig. 3).

III. RESONANT ANTENNA DESIGN

At 55 GHz IMPATT diodes are well suited as active elements on silicon substrates, but demand a resonator resistance below 10 Ω . To build an oscillator, the input impedance of the resonator has to be matched precisely to the IMPATT diode [5].

We calculated the impedance seen by the IMPATT diode using a full wave analysis based on the method of moments in the spectral domain. The electrical field integral equation (EFIE) was used to analyze the impedance of the structure. The EFIE gives the surface current distribution \mathbf{J}_S excited by an incident electric field \mathbf{E}_i by means of dyadic Green's functions $\bar{\bar{G}}^E$ in the space domain [6]. In the spectral domain the EFIE is transformed to

$$\vec{E}_i(\vec{x}) = \frac{1}{4\pi^2} \iint_{-\infty}^{\infty} (\bar{\bar{G}}^E(k_x, k_y) + Z_s) \cdot \tilde{\mathbf{J}}_S(k_x, k_y) e^{-j(k_x x + k_y y)} dk_x dk_y. \quad (1)$$

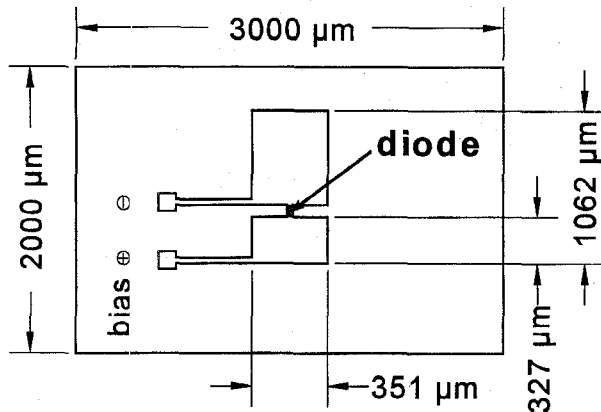


Fig. 2. Layout asymmetric dipole.

In this analysis all the relevant loss phenomena such as dielectric and ohmic losses, radiation, and surface waves have been included.

The method of moments (MoM) is applied to convert the integral equation into a matrix algebraic equation using the subsectional basis function approach. The solution of the resulting complex system matrix delivers all interesting properties of the examined antenna as input impedance, gain, radiation pattern, and radiation efficiency. By examining various different layouts, the asymmetric dipole on a 100-μm silicon substrate with backside metallization (Fig. 2) was found to match the requirements of the IMPATT diode best. By the asymmetric design of the antenna the ratio of resistance to reactance of the antenna has been improved. The negative calculated input impedance of the asymmetric dipole seen by the IMPATT diode versus frequency is depicted in Fig. 3. Since matching is obtained for $Z_{diode} + Z_{dipole} = 0$ the intersection between the negative reactance of the dipole and the reactance of the diode determines the oscillation frequency. With the impedance of dipole and IMPATT diode known by calculation and measurement, respectively, the loaded quality factor is determined to $Q = 14.7$. The radiation efficiency of an antenna is defined as

$$\eta = \frac{\text{power radiated into free space}}{\text{power fed into the antenna}} \quad (2)$$

The calculated $\eta = 51\%$ is within a reasonable range for a planar structure whereas the derived directivity $D = 5.5 \text{ dBi}$ clearly shows the need of an additional beam shaping, e.g. by a dielectric lens.

IV. RESULTS

For the monolithic integrated transmitter, the oscillation frequency has been measured using a spectrum analyzer. For better handling the $2 \times 3 \text{ mm}$ silicon chip with a resistivity of $8000 \Omega/\square$ is mounted on a T039 carrier. The measured oscillation frequency $f = 55.2768 \text{ GHz}$ deviates by only 1.7% from the predicted 56.2 GHz. Additionally, the radiated power P versus the bias current I is depicted in Fig. 4. For measurement of the radiated power P a power meter HP 432A with a V-band thermistor mounted on a standard gain horn

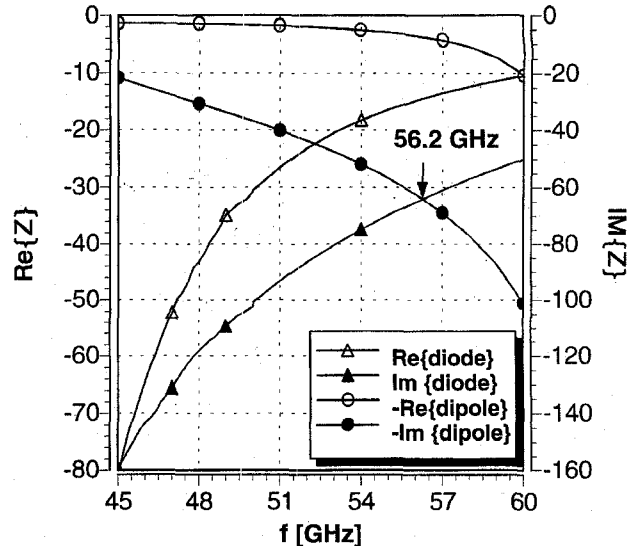
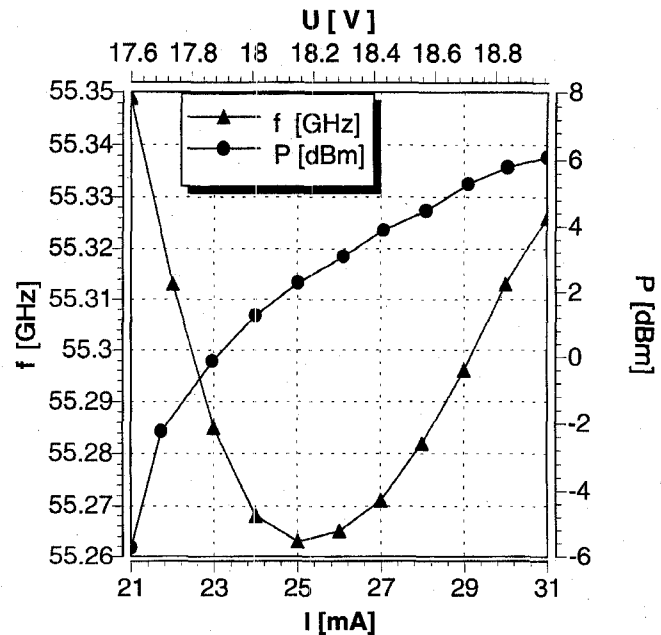


Fig. 3. Impedance of QRDD diode and dipole.

Fig. 4. Oscillation frequency f and radiated power P_{rad} versus bias current I .

antenna has been employed. Subsequently the total radiated power P_{rad} has been calculated using

$$P_{rad} = \frac{P_{meas}}{G_{std}D} \left(\frac{4\pi r}{\lambda_0} \right)^2 \quad (3)$$

where P_{meas} is the power displayed by the power meter, G_{std} is the gain of the standard gain horn antenna, D is the calculated directivity of the asymmetric dipole, and r is the distance of dipole and standard gain horn antenna. While the radiated power is increasing with bias current, the oscillation frequency exhibits a local minimum for a bias current $I = 25 \text{ mA}$. The maximum radiated output power $P_{rad} = 6.1 \text{ dBm}$ at 55.2768 GHz was measured for an applied bias current

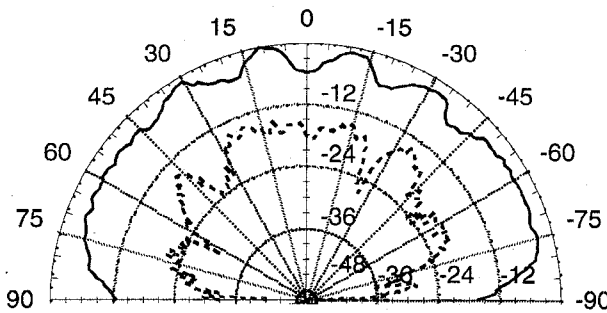


Fig. 5. *E*-plane pattern at $f = 55.342$ GHz. — co-polar. ⋯ x-polar.

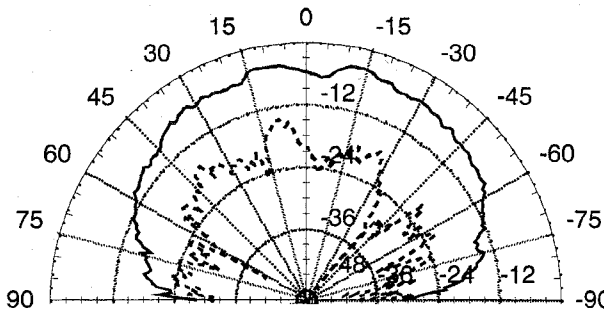


Fig. 6. *H*-plane pattern at $f = 55.342$ GHz. — co-polar. ⋯ x-polar.

of 31 mA and a voltage of 18.97 V. Hence the power P_{gen} generated by the IMPATT diode is determined to

$$P_{gen} = \frac{P_{rad}}{\eta} = 9.1 \text{ dBm} \quad (4)$$

resulting in an efficiency of the diode of 1.4%. By employing an HP 8510 NWA with external harmonic mixers the radiation pattern of the oscillator depicted in Fig. 5 and in Fig. 6 was measured. Due to the 20-MHz intermediate frequency processed by the NWA, the oscillator had to be stabilized by subharmonic injection locking with $f_{sub} = 18.451$ GHz.

The ripple most distinct in the co-polar *E*-plane pattern is induced by the finite extent of the substrate. The orthogonal polarization state in *E*-plane and *H*-plane is suppressed by 12 dB at 0° . The deterioration of the polarization purity that should be better than 20 dB is caused by the dc-feed. By rearranging this feed the polarization purity can be improved substantially.

V. CONCLUSION

By exploiting the resonant characteristics of a planar antenna and directly locating the active element in the planar structure, a self-radiating oscillator has been fabricated. By this configuration, space requirement and parasitic losses of the presented transmitter are reduced to a minimum. Because of reduced size and easy manufacturing, this kind of monolithic integrated transmitter is excellent for low-cost sensor systems in automotive applications.

REFERENCES

- [1] J.-F. Luy, K. M. Strohm, and J. Buechler, "Monolithically integrated coplanar 75 GHz silicon IMPATT oscillator," *Microwave and Optical Technol. Lett.*, vol. 1, pp. 117–119, June 1988.
- [2] A. Stiller, M. Thieme, and E. Biebl, "Polarisationsselektive antennenkonzepte für monolithisch integrierte millimeterwellenschaltungen," *Kleinheubacher Berichte*, Band 38, 1994.
- [3] J.-F. Luy, E. Kasper, and W. Behr, "Semiconductor structures for 100 GHz silicon IMPATT diodes," in *17th Europ. Microwave Conf.*, Rome, 1987, pp. 820–825.
- [4] K. M. Strohm, "Silicon millimeter-wave integrated circuit technology," in *Silicon-Based Millimeter-Wave Devices*, J.-F. Luy and P. Russer, Eds. Berlin: Springer, 1994, pp. 1–46.
- [5] J.-F. Luy, K. M. Strohm, and J. Buechler, "Silicon monolithic millimeter wave IMPATT oscillator," in *Proc. 18th Microwave Conf.*, 1988, pp. 364–369.
- [6] P. Russer and E. Biebl, "Fundamentals," in *Silicon-Based Millimeter-Wave Devices*, J.-F. Luy and P. Russer, Eds. Berlin: Springer, 1994, pp. 1–46.